

A Two-Stage Dual-Modality Model for Facial Emotional Expression Recognition

Jiajun Sun Zhe Gao[†]
Shanghai Normal University

{1000516984@smail.shnu.edu.cn, zgao0911@shnu.edu.cn}

Abstract

This paper addresses the expression (EXPR) recognition challenge in the 10th Affective Behavior Analysis in-the-Wild (ABAW) workshop and competition, which requires frame-level classification of eight facial emotional expressions from unconstrained videos. This challenge presents considerable difficulties stemming from inaccurate face localization, substantial pose and scale variations, motion blur, temporal instability, and other confounding factors prevalent across adjacent frames in video sequences. We propose a two-stage dual-modal (audio–visual) model to handle these difficulties. Stage I focuses on robust visual feature extraction, where a DINOv2-based encoder is designed and pretrained. Specifically, DINOv2 ViT-L/14 is selected as the backbone, a padding-aware augmentation (PadAug) strategy is employed for image padding and data preprocessing from raw videos, and a mixture-of-experts (MoE) training head is integrated to enhance outputs from diversified classifier experts. Stage II addresses modality fusion and temporal consistency. For the visual modality, faces from raw videos are re-cropped at multiple scales, and visual features are extracted from the pretrained DINOv2-based encoder and averaged to form a robust frame-level visual representation. Concurrently, frame-aligned Wav2Vec 2.0 audio features are derived from short audio windows in the same raw videos to provide complementary acoustic cues. These dual-modal features are integrated via a lightweight gated fusion module, followed by inference-time temporal smoothing to enhance both accuracy and temporal consistency for facial expression predictions. Experiments on the ABAW dataset demonstrate the effectiveness and efficiency of the proposed method. The two-stage model achieves a Macro-F1 score of 0.5368 on the official validation set and 0.5122 ± 0.0277 under 5-fold cross-validation. Both results outperform the official baselines, demonstrating the effectiveness of the proposed method for robust facial emotion recognition under challenging raw video conditions.

1. Introduction

Facial emotional expression recognition (EXPR) from audiovisual datasets in unconstrained environments (i.e., *in-the-wild*) is an important task in Affective & Behavioral Analysis. In recent years, the EXPR task has attracted increasing attention owing to its broad applications across diversified fields, e.g., human–computer interaction, affective computing, and behavioral analysis. To advance EXPR research, significant benchmarks have been established, notably Aff-Wild and Aff-Wild2, alongside the ABAW workshop and competition series [1–12].

The 10th ABAW workshop in 2026 continues this line of research, and the EXPR track this year requires classifying each raw video frame in the Aff-Wild2 dataset into one of eight categories: Neutral, Anger, Disgust, Fear, Happiness, Sadness, Surprise, and Other [3, 11–13]. Consequently, robust frame-level expression recognition is required.

However, compared with controlled laboratory settings, real-world scenarios present substantial challenges for accurate and consistent facial emotional EXPR recognition. In raw videos of Aff-Wild2, for instance, face localization is often inaccurate or unstable, facial scale may vary substantially across frames, and many samples are affected by blur, occlusion, extreme pose, illumination changes, or low image quality [2, 3, 14]. These issues make visual evidence noisy and inconsistent across time and hence complicate reliable emotion perception from individual frames.

In addition, affective signals in real-world audiovisual data are naturally multimodal. The visual modality, e.g., face appearance, alone may not be sufficient in ambiguous situations, while complementary cues from the audio modality, e.g., speech, can provide additional but critical information. However, effectively integrating audio and visual information remains challenging, especially when frame-level predictions fluctuate over time due to noisy observations. To address these challenges, we propose a two-stage dual-modality (audio–visual) framework for robust affective perception from raw *in-the-wild* videos.

Stage I: Visual adaptation. We adapt a pretrained DINOv2-based encoder for robust visual feature extraction from raw videos [15]. Specifically, DINOv2 ViT-L/14 is

trained with a padding-aware augmentation (PadAug) strategy to simulate crop-boundary artifacts while preserving facial content. In addition, an MoE-based MLP head is introduced during training to enhance task adaptation and feature diversity. After training on Aff-Wild2 and AffectNet+, only the adapted DINOv2 backbone is retained to provide expression-aware visual representations for the next stage [3, 16, 17].

Stage II: Frame-level dual-modality emotion recognition. Using the adapted visual encoder from Stage I, we perform frame-level audio-visual expression recognition on raw videos. For each frame, three-scale face crops are extracted and encoded by DINOv2, and their averaged features form the visual representation. In parallel, frame-aligned acoustic features are extracted using Wav2Vec 2.0 [18]. The two modalities are then fused by a lightweight gated fusion module, followed by inference-time temporal smoothing to improve prediction stability and temporal consistency.

We evaluate our model on Aff-Wild2, the official ABAW dataset [3, 11, 12]. Our model achieves 0.5368 Macro-F1 on the official validation set and 0.5122 ± 0.0277 Macro-F1 under 5-fold cross-validation. Both results are substantially better than the baseline and rank among the top-performing methods compared with those from previous competitions. These results demonstrate the superiority of our model in handling complex challenges in *in-the-wild* audiovisual datasets, achieving high EXPR accuracy, smoother temporal consistency, more stable prediction reliability, and a lighter model size in terms of the number of parameters.

Contributions. Four Contributions can be summarized:

- Develop a competitive method for EXPR via audiovisual dataset in-the-wild based on a two stage dual modality framework which utilizes as comprehensive information as possible for challenging settings and return remarked emotional recognition results.
- Propose a padding-aware augmentation data preprocessing strategy to eliminate gaps between frame level facial emotional expressions and raw videos, alleviating performance sensitivity to crop boundaries and improving model robustness for multi-scale facial inputs.
- Adopt a two-stage model architecture with stage-specific focuses. Stage I emphasizes data preprocessing and visual feature, providing core evidence from the raw videos for emotion detection. Stage II solves the parallel modality integration with supplemented acoustic cues and feature filtering with a gate module. This two-stage design returns cutting-edge performance and dramatically reduces computational complexity as well.
- Select a simple yet effective inference-time temporal smoothing method to improve frame-level prediction con-

sistency and enhance the model robustness on audiovisual data in-the-wild.

2. Related Work

2.1. EXPR in the Wild

Frame-level facial expression recognition in the wild (EXPR) aims to predict dense expression labels from unconstrained video frames, and has become a central task in affective computing with the development of the Aff-Wild/Aff-Wild2 benchmarks and the ABAW challenge series [1–13, 19]. Compared with controlled settings, EXPR in the wild is considerably more challenging due to large variations in head pose, illumination, occlusion, motion blur, face scale, and annotation noise across long video sequences. To improve robustness under such conditions, Gera *et al.* [20] studied in-the-wild expression recognition under the ABAW setting, while Savchenko and Sidorova [21] combined pretrained facial encoders with temporal convolutional modeling to better exploit contextual information across frames; recent ABAW submissions further explored audio-visual and temporal designs for expression recognition in the wild [22, 23]. Despite these advances, reliable frame-level EXPR remains difficult when face crops are imperfect and facial scales vary significantly across video frames, which is common in raw videos collected in real-world environments.

2.2. Modelling for EXPR

Facial expression recognition (EXPR) has been extensively studied with deep neural networks. Early methods mainly relied on CNN-based models trained on image-level FER datasets [24–26], while recent works introduced stronger transformer-based architectures for improved visual modeling [21, 27–29]. For video-based EXPR, prior studies further incorporated temporal modeling and audio-visual fusion to exploit temporal continuity and multimodal complementarity [22, 23, 30–36]. Nevertheless, robust EXPR in the wild remains challenging due to noise in both modalities and unstable frame-level observations. Our method therefore combines a strengthened visual encoder with lightweight multimodal fusion for stable frame-level prediction.

2.3. Modality fusion for emotion EXPR

Because facial and vocal signals provide complementary affective cues, multimodal fusion has been widely explored in ABAW and related in-the-wild emotion recognition studies. Existing methods typically extract visual and audio representations separately and then combine them through feature concatenation, probability-level fusion, cross-modal attention, or other interaction mechanisms. For example, Kim *et al.* [35] adopted a cascaded cross-attention trans-

former for multimodal fusion, while recent ABAW systems also explored pretrained unimodal features followed by lightweight or attention-based fusion designs [9, 11, 22, 23]. Overall, prior work suggests that effective multimodal learning depends not only on the quality of unimodal representations, but also on how complementary cues are selectively integrated under noisy real-world conditions. Motivated by this observation, we are particularly interested in whether a lightweight gating-based filtering mechanism can help emphasize informative cross-modal cues while suppressing less reliable ones during fusion.

2.4. Temporal smoothing

Temporal modeling is another important component in video-based emotion recognition, since neighboring frames are usually correlated and instantaneous predictions can be unstable in unconstrained videos. Existing studies have introduced temporal convolution, transformer-based interaction, semi-temporal learning, or other sequential refinement strategies to capture contextual information across time [9, 11, 21, 35, 36]. From a broader perspective, affect has often been described as a continuously evolving process rather than a sequence of fully independent states, as reflected by the circumplex model of affect [37]. Although EXPR is formulated as discrete frame-level classification, this view still suggests that temporal continuity and expression duration should be taken into account when modeling predictions in the wild. Considering the combined challenges of visual corruption, multimodal complementarity, and temporal continuity, we therefore adopt a two-stage framework that decouples unimodal feature extraction from subsequent multimodal and temporal modeling.

3. Method

As illustrated in Fig. 1, our method performs frame-level audio-visual expression recognition from raw videos in a two-stage manner. For each target frame, we re-crop the face directly from the raw video and construct three facial crops with different scales, which are encoded by a DINOv2 visual backbone to obtain a robust multi-scale visual representation. In parallel, a short audio segment centered at the target frame is encoded by Wav2Vec 2.0 to produce a frame-aligned acoustic representation. The visual and audio features are then integrated by a lightweight gated fusion module for frame-level expression classification, and a simple temporal smoothing step is applied during inference to improve prediction stability and temporal consistency.

The visual encoder in Fig. 1 is initialized from a pretrained DINOv2 model and further adapted through the Stage-I pipeline shown in Fig. 2. Specifically, Stage I adapts DINOv2 on two image-level FER datasets, AffectNet and RAF-DB, using padding-aware augmentation (PadAug) together with a training-only mixture-of-experts (MoE) head.

After adaptation, the MoE head is discarded and only the adapted DINOv2 backbone is retained for Stage-II audio-visual learning on raw videos. Overall, this two-stage design improves the expression sensitivity of the visual encoder before multimodal fusion and offers a practical alternative to end-to-end optimization on long unconstrained videos.

3.1. Stage-I Visual Adaptation

To improve the expression sensitivity of the visual encoder before multimodal learning, we adapt DINOv2 on two image-level FER datasets, AffectNet [16] and RAF-DB [26]. These datasets provide large-scale supervision for learning discriminative expression features under diverse facial appearances. Since the final target task is frame-level EXPR recognition in unconstrained videos, this intermediate adaptation serves as an efficient bridge between generic self-supervised visual pretraining and video-based expression analysis.

3.1.1. Padding-aware Augmentation (PadAug)

A practical issue in our setting is that large facial crops may exceed the image boundary, especially when larger crop scales are used. In such cases, padded regions appear near the image borders, introducing a non-negligible distribution shift between visually clean training images and boundary-affected face crops encountered later in raw-video inference, as illustrated in Fig. 3.

To alleviate this mismatch, we introduce a padding-aware augmentation strategy termed *PadAug*. During Stage-I adaptation, PadAug randomly inserts black padding bars along image boundaries and applies small spatial perturbations to the padded region. As shown in Fig. 3, the augmentation simulates several common boundary conditions, including left, right, top, and bottom padding, as well as corner-like artifacts. The purpose is to explicitly expose the model to the boundary patterns commonly produced by large-scale face cropping in unconstrained videos. Unlike generic data augmentation, PadAug is tailored to the scale-variation and boundary-corruption problem in multi-scale facial representation learning.

3.1.2. MoE-assisted DINOv2 Adaptation

DINOv2 ViT-L/14 [15] is adopted as the visual backbone for strong transferable visual representations. Given an input face image x , the backbone outputs a CLS-token feature

$$u = E_v(x), \quad u \in \mathbb{R}^{1024}, \quad (1)$$

where $E_v(\cdot)$ denotes the DINOv2 encoder.

During Stage-I adaptation, we freeze the patch embedding layer and keep the early transformer blocks fixed, while updating the deeper layers to specialize the representation for facial expression recognition. In the final setting,

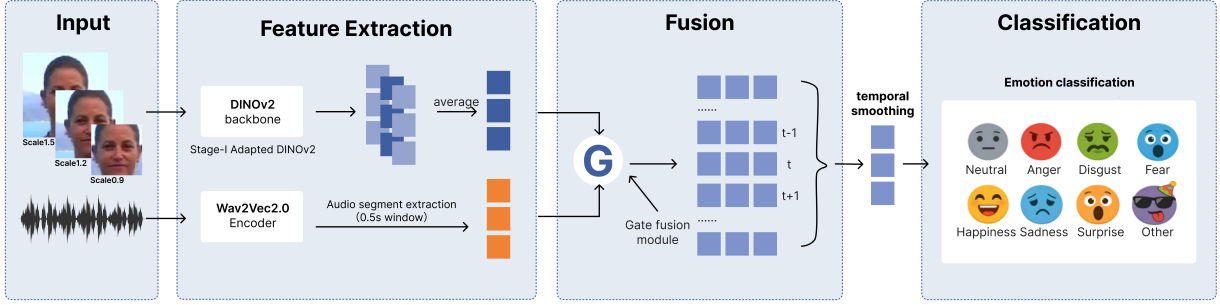


Figure 1. The overview of our proposed model. For each target frame, three facial crops with different scales are extracted from the raw video and encoded by a DINOv2 backbone that has been pre-adapted in Stage I (see Fig. 2). The resulting multi-scale visual representation is fused with a frame-aligned Wav2Vec 2.0 audio representation through a gated fusion module for frame-level expression recognition. During inference, lightweight temporal smoothing is further applied to improve prediction stability and temporal consistency.

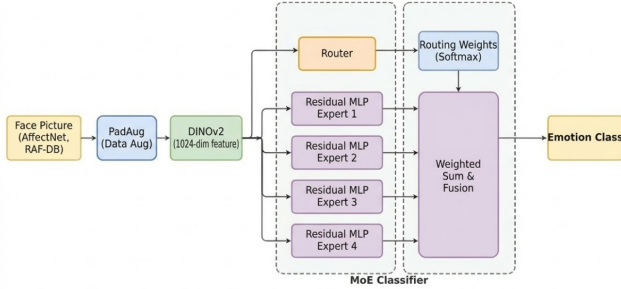


Figure 2. The DINOv2-based encoder, AffectNet and RAF-DB. PadAug is used to simulate boundary padding artifacts caused by large facial crops, while a training-only MoE task head provides sample-dependent expert routing to enhance DINOv2 adaptation. After Stage I, the MoE head is discarded and only the adapted DINOv2 backbone is retained 1.

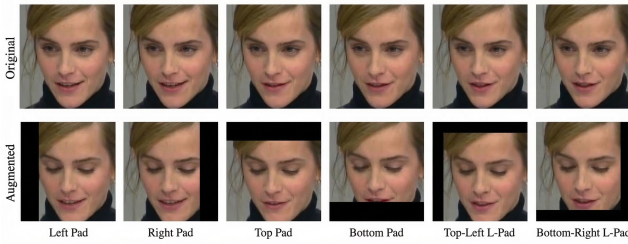


Figure 3. Illustration of the proposed padding-aware augmentation (PadAug). The top row shows original facial crops, while the bottom row presents augmented samples where artificial padding is applied to different image boundaries to simulate boundary artifacts caused by imperfect face cropping in raw videos.

the first eight transformer blocks are frozen. This partial fine-tuning strategy preserves strong generic visual priors while still allowing high-level facial semantics to adapt to

the expression domain.

To provide stronger task-oriented supervision during adaptation, we attach a training-only MoE classifier to the DINOv2 feature u . The MoE head contains a router and multiple expert branches. The normalized feature is fed into the router to generate sample-dependent expert weights:

$$\alpha = \text{softmax}(R(\text{LN}(u))), \quad (2)$$

where $R(\cdot)$ denotes the routing function and $\alpha \in \mathbb{R}^M$ is the routing weight over M experts. Each expert is implemented as an MLP-based transformation. The expert outputs are aggregated by weighted summation:

$$\tilde{u} = \sum_{m=1}^M \alpha_m e_m. \quad (3)$$

The final logits are then produced by a normalization-dropout-linear classification layer:

$$\ell = W_c \text{Drop}(\text{LN}(\tilde{u})) + b_c. \quad (4)$$

Compared with a standard single-branch classifier, the MoE head allows different experts to specialize in different expression patterns and provides richer supervisory signals for adapting the visual backbone. Importantly, the MoE head is used only during Stage I. After adaptation, it is discarded, and only the adapted DINOv2 backbone is retained for feature extraction in Stage II.

3.1.3. Stage-I Objective

The objective function in Stage I is to minimize a class-weighted cross-entropy loss, and the loss is calculated as:

$$\mathcal{L}_{\text{stage1}} = - \sum_{c=1}^C w_c \tilde{y}^{(c)} \log p^{(c)}, \quad (5)$$

where $p^{(c)}$ denotes the predicted probability for class c , w_c denotes the corresponding class weight, \tilde{y} is a soft target distribution, and $C = 8$ is the number of expression categories.

3.2. Stage-II Frame-level Audio–Visual Modeling on Aff-Wild2

After Stage-I adaptation, we apply the adapted visual encoder to the ABAW EXPR task on Aff-Wild2. Stage II focuses on frame-level multimodal modeling rather than further heavy backbone adaptation. Specifically, we construct a multi-scale visual representation for each frame, align an acoustic representation to the same temporal position, and train a lightweight gated fusion head for expression recognition.

3.2.1. Raw-video Face Re-cropping and Multi-scale Visual Features

The official ABAW face crops are relatively low-resolution, which may weaken subtle expression cues after resizing. To preserve more fine-grained facial details, we re-crop faces directly from the raw video frames and resize each crop to the input resolution required by DINOv2.

For each target frame t , we construct three facial crops at different scales, corresponding to scale factors 0.9, 1.2, and 1.5. Let $x_t^{(s)}$ denote the crop at scale s . The adapted DINOv2 backbone extracts a feature for each scale:

$$f_t^{v,s} = E_v(x_t^{(s)}). \quad (6)$$

The final frame-level visual representation is obtained by simple averaging across scales:

$$f_t^v = \frac{1}{3} \sum_{s \in \{0.9, 1.2, 1.5\}} f_t^{v,s}. \quad (7)$$

This design provides complementary information from different crop extents while keeping the visual branch lightweight.

3.2.2. Frame-aligned Audio Features

To provide complementary affective cues from speech, we extract acoustic features using Wav2Vec 2.0 Large [18]. Since audio and video have different temporal resolutions, frame-level alignment is required before multimodal fusion.

For each target frame t , we use a short audio segment centered around the frame and aggregate the corresponding acoustic features to form a frame-level audio representation. Let z_τ denote the acoustic feature at temporal index τ , and let Ω_t denote the set of indices aligned with frame t . The aligned audio feature is defined as

$$f_t^a = \frac{1}{|\Omega_t|} \sum_{\tau \in \Omega_t} z_\tau. \quad (8)$$

In the final system, we use a centered temporal window of 0.50s for this aggregation. This short-window averaging provides more stable acoustic cues than direct nearest-neighbor assignment.

3.2.3. Gated Audio–Visual Fusion

Given the visual feature f_t^v and the audio feature f_t^a , we fuse them through a lightweight gated fusion module. First, the two modalities are projected into a shared hidden space:

$$z_t^v = P_v(f_t^v), \quad z_t^a = P_a(f_t^a), \quad (9)$$

where $P_v(\cdot)$ and $P_a(\cdot)$ are learnable linear projections for the visual and audio branches, respectively.

A gating vector is then predicted from the concatenated raw features:

$$g_t = \sigma(G([f_t^v; f_t^a])), \quad (10)$$

where $G(\cdot)$ denotes the gating network, $[\cdot; \cdot]$ denotes concatenation, and $\sigma(\cdot)$ is the sigmoid activation. The fused representation is computed as

$$h_t = g_t \odot z_t^v + (1 - g_t) \odot z_t^a, \quad (11)$$

where \odot denotes element-wise multiplication.

The final frame-level logits are obtained by a normalization–dropout–classification head:

$$\ell_t = W_o \text{Drop}(\text{LN}(h_t)) + b_o. \quad (12)$$

This formulation allows the model to adaptively control the relative contribution of visual and acoustic cues according to their frame-wise reliability.

3.2.4. Stage-II Objective

Stage II is trained on the Aff-Wild2 EXPR labels using the frame-level multimodal representations described above. Since the visual backbone has already been adapted in Stage I and the acoustic encoder is pretrained, Stage II only needs to optimize a lightweight fusion head, which substantially reduces the training cost of multimodal learning.

Let $p_t^{(c)}$ denote the predicted probability for class c at frame t , and let y_t denote the ground-truth label. We optimize a class-weighted cross-entropy loss over valid labeled frames:

$$\mathcal{L}_{\text{stage2}} = - \sum_{c=1}^C w_c \mathbf{1}(y_t = c) \log p_t^{(c)}, \quad (13)$$

where w_c is the class weight for class c . This objective encourages discriminative multimodal representations while partially alleviating class imbalance.

3.2.5. Inference-time Temporal Smoothing

Although classification is performed at the frame level, adjacent video frames usually exhibit strong temporal continuity. Direct frame-wise predictions may therefore fluctuate due to blur, occlusion, weak facial evidence, or noisy audio. To improve temporal consistency without introducing an additional temporal backbone, we apply lightweight post-hoc temporal smoothing during inference. After carefully comparing in an ablation study, the median smoothing method is selected. Detailed of the comparison is displayed in Section 4.

Let $\ell_t \in \mathbb{R}^C$ denote the predicted logit vector for frame t , where $C = 8$ is the number of expression classes. We consider a temporal window centered at frame t :

$$\mathcal{N}(t) = \{t - k, \dots, t, \dots, t + k\}, \quad (14)$$

where the window size is $2k + 1$. In the final system, we use an odd window size of 101 frames.

The smoothed logit for class c is defined as

$$\tilde{\ell}_{t,c} = \text{median}(\ell_{t-k,c}, \dots, \ell_{t+k,c}), \quad (15)$$

the final prediction is then obtained by

$$\tilde{y}_t = \arg \max_c \tilde{\ell}_{t,c}. \quad (16)$$

4. Experiments and Results

4.1. Evaluation Metric

Following the ABAW EXPR challenge protocol [38], we use the official EXPR score, namely the macro-averaged F_1 score over all expression categories, as the main evaluation metric. Let C denote the number of expression categories. The overall EXPR score is defined as

$$P_{\text{EXPR}} = \frac{1}{C} \sum_{c=1}^C F_1^{(c)}, \quad (17)$$

where $F_1^{(c)}$ denotes the F_1 score of the c -th expression category. For each class, the F_1 score is computed as

$$F_1^{(c)} = \frac{2 \times \text{precision}_c \times \text{recall}_c}{\text{precision}_c + \text{recall}_c}, \quad (18)$$

where precision_c and recall_c denote the precision and recall of class c , respectively. In this work, $C = 8$, corresponding to the seven basic expressions and an additional *other* category. Although the models are optimized with cross-entropy-based objectives, all major comparisons in this paper are reported using the macro-averaged F_1 score.

4.2. Experimental Settings

Our experiments follow the two-stage design in Section 3. For the visual branch, we use DINOv2 ViT-L/14 initialized from the official self-supervised pretrained checkpoint and adapt it to facial expression recognition in Stage I. For the audio branch, we use wav2vec 2.0 large-lv60k ASR. In Stage I, DINOv2 ViT-L/14 is trained on image-level FER datasets with the proposed visual adaptation strategy, which combines PadAug with a training-only MoE head. We freeze the first eight transformer blocks and optimize the remaining layers for 12 epochs using AdamW, with a backbone learning rate of 1×10^{-5} and a head learning rate of 3×10^{-4} . Mixup, label smoothing, and class-balanced supervision are also applied, and the best checkpoint is selected according to the validation macro-averaged F_1 score. In Stage II, for the ABAW EXPR task on Aff-Wild2, we build a three-scale visual representation using face crops with scales 0.9, 1.2, and 1.5, and average the corresponding DINOv2 features. Frame-aligned wav2vec 2.0 features are extracted with a centered temporal window of 0.50 s, and a lightweight gated fusion model is trained on frame-level labels. Inference-time temporal smoothing is further evaluated with a fixed window size of 101 frames.

4.3. Overall Results

Before presenting the component-wise ablations, we first summarize the performance of the final system. The final configuration adopts raw-video face re-cropping with multi-scale visual inputs (0.9/1.2/1.5), a DINOv2 ViT-L/14 backbone adapted by MoE-assisted fine-tuning with PadAug, Wav2Vec 2.0 audio features aligned by a 0.50 s window mean, gated fusion for audio-visual integration, and median filtering with a temporal window size of 101 during inference.

Starting from the best visual-only setting, which achieves a macro-averaged F_1 score of 0.4344 on the official validation set, introducing audio-visual gated fusion improves the score to 0.5131 and yields a 5-fold mean score of 0.4842. After applying inference-time temporal smoothing, the final system further reaches 0.5368 on the official validation set and 0.5122 ± 0.0277 under 5-fold cross-validation. These results indicate that the overall gain comes from the combination of stronger visual adaptation, effective multimodal fusion, and lightweight temporal post-processing. The following subsections analyze each component in detail.

4.4. Ablation on Multi-scale Face Representation and Visual Training

Table 1 compares different face crop settings and visual training strategies. Re-cropped faces from raw videos consistently outperform the official face crops, suggesting that the official low-resolution crops lose useful facial details

Table 1. Ablation on face crop scale and visual encoder training strategy. Results are reported as F1 on the official validation set using a linear classifier on top of the extracted frozen visual features.

Training Method	Official Face Crop + Linear	FaceCrop-0.9 + Linear	FaceCrop-1.2 + Linear	FaceCrop-1.5 + Linear	Multi-scale Mean (0.9/1.2/1.5) + Linear
Pretrained	0.3007	0.3199	0.3307	0.3192	0.3355
Fine-tune + MLP	0.3378	0.3697	0.3773	0.3738	0.3800
Fine-tune + MoE	0.3576	0.4040	0.4251	0.4223	0.4257
Fine-tune + MoE + PadAug	0.3525	0.3992	0.4205	0.4245	0.4344

Table 2. Ablation on audio-frame alignment strategy. Results are reported as F1 on the official validation set.

Alignment Strategy	F1
Nearest	0.2423
Window Mean (0.25 s)	0.2876
Window Mean (0.50 s)	0.2901
Window Mean (0.75 s)	0.2886

after resizing. Under the same training strategy, averaging three crop scales (0.9/1.2/1.5) performs better than any single-scale input, indicating that multi-scale representation provides complementary information. In addition, task-specific fine-tuning clearly improves over directly using pretrained DINOv2 features, and replacing a standard MLP head with an MoE head brings further gains, showing the benefit of stronger task adaptation. The best result is obtained by combining MoE with PadAug under multi-scale inputs, reaching a macro-averaged F_1 score of **0.4344**. Notably, the largest crop scale (1.5) becomes more competitive after PadAug, suggesting that explicitly simulating boundary padding helps reduce the distribution shift caused by large-scale crops.

4.5. Ablation on Audio Alignment Strategy

Table 2 studies how audio features are aligned with video frames. Direct nearest-neighbor assignment gives relatively weak performance, whereas temporal window averaging consistently improves the macro-averaged F_1 score, indicating that short-term acoustic context is more informative than a single aligned audio instant. Among all tested settings, averaging audio features within a 0.50s window achieves the best result of **0.2901**, suggesting that moderate temporal aggregation is sufficient to capture useful speech dynamics without introducing excessive smoothing. Therefore, we adopt the 0.50s window mean strategy in the final system.

4.6. Ablation on Audio–Visual Fusion

After fixing the visual and audio representations, we compare several fusion strategies in Table 3. All multimodal fusion methods outperform the unimodal baselines, indicating that audio provides complementary cues beyond the visual stream alone. Even the simplest *Concat + Linear* base-

line improves the F_1 score from 0.4344 for the visual-only model to 0.4717 on the official validation set.

More expressive fusion modules generally perform better, although their gains are not solely determined by parameter count. For example, bilinear fusion and dynamic weighting are both more complex than simple concatenation, yet their improvements remain limited. Among all methods, *Gated Fusion* achieves the best official validation F_1 score of **0.5131** and the best 5-fold mean F_1 score of **0.4842**. Although *Cross-modal Attention* is competitive, it introduces substantially more parameters (6.31M vs. 2.37M). Considering both effectiveness and complexity, we adopt gated fusion as the default multimodal fusion module in the final system.

4.7. Ablation on Temporal Smoothing

Frame-level predictions in unconstrained videos are often unstable due to ambiguous expressions, occlusion, motion blur, and abrupt pose changes. We therefore evaluate several inference-time temporal smoothing strategies, including mean smoothing, median filtering, Gaussian weighting, and hard voting. We perform a window-size ablation on the validation set by varying the temporal window from 3 to 205 frames with a step size of 2. Figure 4 shows the performance trend under different window sizes, while Table 4 reports the final comparison using a fixed window size of 101 frames.

All smoothing strategies improve the macro-averaged F_1 score compared with the single-frame baseline, indicating that enforcing short-range temporal consistency helps stabilize predictions even without an explicit temporal backbone. The best performance is achieved when the window size is around 100 frames. Among all strategies, *Median Filter* achieves the highest performance, reaching **0.5368** on the official validation set and 0.5122 ± 0.0277 under 5-fold cross-validation. Therefore, median smoothing with a window size of 101 is adopted in the final system.

4.8. Discussion

The results suggest that the main performance gains come from a progressive design rather than a single complex component. In Stage I, visual adaptation improves the robustness of frame-level expression features under raw-video conditions. In Stage II, multimodal fusion further enhances performance by incorporating complementary audio cues,

Table 3. Comparison of different audio–visual fusion strategies. Results are reported as F1 on the official validation set and under 5-fold cross-validation.

Fusion	Params	Official Val F1	5-Fold Mean F1	Fold-1	Fold-2	Fold-3	Fold-4	Fold-5
A only	–	0.2901	–	–	–	–	–	–
V only	–	0.4344	–	–	–	–	–	–
Concat + Linear	16K	0.4717	0.4527	0.4527	0.4203	0.4629	0.4946	0.4331
Concat + MLP	1.05M	0.5079	0.4838	0.4670	0.4725	0.4983	0.5340	0.4474
Bilinear	1.32M	0.4794	0.4502	0.4312	0.4341	0.4670	0.4714	0.4472
Dynamic Weighting	2.10M	0.4712	0.4558	0.4466	0.4442	0.4651	0.4672	0.4557
Gated Fusion	2.37M	0.5131	0.4842	0.4713	0.4783	0.4892	0.5235	0.4614
Cross-modal Attention	6.31M	0.5099	0.4837	0.4665	0.4702	0.4759	0.5112	0.4947

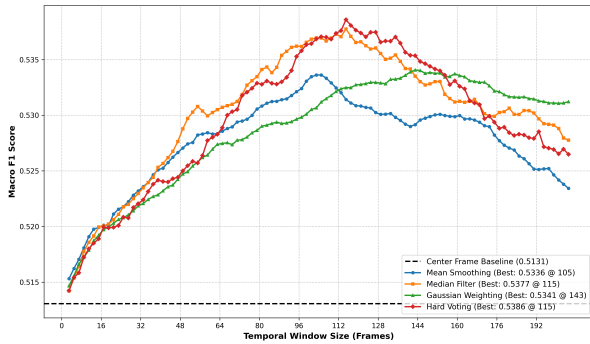


Figure 4. Macro-averaged F_1 score under different temporal smoothing strategies and window sizes.

Table 4. Temporal smoothing results with a fixed window size of 101. Results are reported as F1 on the official validation set and under 5-fold cross-validation.

Strategy	Official Val F1	5-Fold Mean F1 \pm Std
Single-frame Baseline	0.5131	0.4842 \pm 0.0212
Mean Smoothing	0.5335	0.5114 \pm 0.0303
Median Filter	0.5368	0.5122 \pm 0.0277
Gaussian Weighting	0.5305	0.5098 \pm 0.0273
Hard Voting	0.5364	0.5095 \pm 0.0258

while temporal smoothing provides an additional improvement by enforcing short-range prediction consistency. This staged formulation is simple, effective, and practical for the ABAW setting.

Another important observation is that lightweight design choices are sufficient to obtain strong validation performance. Instead of relying on a heavy temporal backbone, our system combines adapted visual representations, aligned audio features, and a simple post-hoc smoothing strategy. This keeps the framework easy to train and extend, while still yielding consistent gains on the official validation set. These findings indicate that, for in-the-wild expression recognition, robust visual adaptation and stable multimodal

integration may be more critical than overly complicated temporal modeling.

5. Conclusion and Future Work

5.1. Conclusion

This paper addresses the EXPR track of the 10th ABAW challenge with a lightweight two-stage audio–visual framework. In Stage I, a pretrained DINOv2 ViT-L/14 backbone is adapted on AffectNet and RAF-DB using PadAug and a training-only MoE head to obtain a more robust expression-aware visual encoder. In Stage II, the adapted visual encoder is combined with frame-aligned wav2vec 2.0 acoustic features through lightweight gated fusion, together with inference-time temporal smoothing for more stable predictions.

Experiments show that these components are complementary. Gated audio–visual fusion improves the official validation macro-averaged F_1 score from 0.4344 to 0.5131, and temporal smoothing further raises the final performance to **0.5368** on the official validation set and 0.5122 ± 0.0277 under 5-fold cross-validation. These results demonstrate the effectiveness of combining stronger visual adaptation, lightweight multimodal fusion, and simple temporal post-processing for in-the-wild facial expression recognition.

5.2. Future Work

Future work will explore stronger visual modeling and more effective multimodal learning. In particular, adaptive face re-cropping, scale-aware feature aggregation, and finer-grained facial region modeling may further improve visual robustness, while lightweight audio adaptation and better temporal aggregation may strengthen the contribution of the audio branch. It is also promising to extend the framework to joint learning of EXPR, valence–arousal, and action units for more general and robust affective representation learning in the wild.

References

- [1] S. Zafeiriou, D. Kollias, M. A. Nicolaou, A. Papaioannou, G. Zhao, and I. Kotsia, "Aff-wild: Valence and arousal 'in-the-wild' challenge," in *Proceedings of the IEEE Conference on Computer Vision and Pattern Recognition Workshops*, pp. 1980–1987, 2017. 1, 2
- [2] D. Kollias, P. Tzirakis, M. A. Nicolaou, A. Papaioannou, G. Zhao, B. Schuller, I. Kotsia, and S. Zafeiriou, "Deep affect prediction in-the-wild: Aff-wild database and challenge, deep architectures, and beyond," *International Journal of Computer Vision*, pp. 1–23, 2019. 1
- [3] D. Kollias and S. Zafeiriou, "Aff-wild2: Extending the aff-wild database for affect recognition," *arXiv preprint arXiv:1811.07770*, 2018. 1, 2
- [4] D. Kollias, A. Schulc, E. Hajiyev, and S. Zafeiriou, "Analysing affective behavior in the first abaw competition," in *IEEE International Conference on Automatic Face and Gesture Recognition*, 2020.
- [5] D. Kollias and S. Zafeiriou, "Analysing affective behavior in the second abaw2 competition," in *IEEE/CVF International Conference on Computer Vision*, 2021.
- [6] D. Kollias, "Abaw: Valence-arousal estimation, expression recognition, action unit detection & multi-task learning challenges," in *Proceedings of the IEEE/CVF Conference on Computer Vision and Pattern Recognition*, pp. 2328–2336, 2022.
- [7] D. Kollias, "Abaw: Learning from synthetic data & multi-task learning challenges," in *European Conference on Computer Vision*, pp. 157–172, Springer, 2023.
- [8] D. Kollias, P. Tzirakis, A. Baird, A. Cowen, and S. Zafeiriou, "Abaw: Valence-arousal estimation, expression recognition, action unit detection & emotional reaction intensity estimation challenges," in *Proceedings of the IEEE/CVF Conference on Computer Vision and Pattern Recognition*, pp. 5888–5897, 2023.
- [9] D. Kollias, P. Tzirakis, A. Cowen, and S. Zafeiriou, "The 6th affective behavior analysis in-the-wild (abaw) competition," in *IEEE/CVF Conference on Computer Vision and Pattern Recognition*, 2024. 3
- [10] D. Kollias, S. Zafeiriou, I. Kotsia, and A. Dhall, "7th abaw competition: Multi-task learning and compound expression recognition," in *European Conference on Computer Vision*, 2024.
- [11] D. Kollias, P. Tzirakis, A. Cowen, and S. Zafeiriou, "Advancements in affective and behavior analysis: The 8th abaw workshop and competition," in *IEEE/CVF Conference on Computer Vision and Pattern Recognition*, 2025. 1, 2, 3
- [12] D. Kollias and S. Zafeiriou, "From emotions to violence: Multimodal fine-grained behavior analysis at the 9th abaw," in *IEEE/CVF International Conference on Computer Vision*, 2025. 1, 2
- [13] D. Kollias and S. Zafeiriou, "Expression, affect, action unit recognition: Aff-wild2, multi-task learning and arcfac," *arXiv preprint arXiv:1910.04855*, 2019. 1, 2
- [14] D. Kollias and S. Zafeiriou, "Affect analysis in-the-wild: Valence-arousal, expressions, action units and a unified framework," *arXiv preprint arXiv:2103.15792*, 2021. 1
- [15] M. Oquab, T. Darcet, and T. Moutakanni, "Dinov2: Learning robust visual features without supervision," *arXiv preprint arXiv:2304.07193*, 2023. 1, 3
- [16] A. Mollahosseini, B. Hasani, and M. H. Mahoor, "Affectnet: A database for facial expression, valence, and arousal computing in the wild," *IEEE Transactions on Affective Computing*, vol. 10, no. 1, pp. 18–31, 2017. 2, 3
- [17] A. P. Fard, M. M. Hosseini, T. D. Sweeny, and M. H. Mahoor, "Affectnet+: A database for enhancing facial expression recognition with soft-labels," *IEEE Transactions on Affective Computing*, pp. 1–16, 2025. 2
- [18] A. Baevski, Y. Zhou, and A. Mohamed, "wav2vec 2.0: A framework for self-supervised learning of speech representations," *Advances in Neural Information Processing Systems*, 2020. 2, 5
- [19] D. Kollias, S. Zafeiriou, I. Kotsia, P. Tzirakis, A. Cowen, E. Granger, M. Pedersoli, and S. Bacon, "10th workshop and competition on affective & behavior analysis in-the-wild (abaw)." Official workshop and competition website, in conjunction with IEEE/CVF CVPR 2026, 2026. Accessed: 2026-03-10. 2
- [20] D. Gera, B. N. S. Kumar, B. V. Raj Kumar, and S. Balasubramanian, "Abaw: Facial expression recognition in the wild," *arXiv preprint arXiv:2303.09785*, 2023. 2
- [21] A. V. Savchenko and A. P. Sidorova, "Emotiefnet and temporal convolutional networks in video-based facial expression recognition and action unit detection," in *Proceedings of the IEEE/CVF Conference on Computer Vision and Pattern Recognition (CVPR) Workshops*, pp. 4849–4859, 2024. 2, 3
- [22] D. Dresvyanskiy, M. Markitantov, J. Yu, P. Li, H. Kaya, and A. Karpov, "Sun team's contribution to abaw 2024 competition: Audio-visual valence-arousal estimation and expression recognition," *arXiv preprint arXiv:2403.12609*, 2024. 2, 3
- [23] A. V. Savchenko, "Hsemotion team at abaw-8 competition: Audiovisual ambivalence/hesitancy, emotional mimicry intensity and facial expression recognition," *arXiv preprint arXiv:2503.10399*, 2025. 2, 3
- [24] A. Mollahosseini, D. Chan, and M. H. Mahoor, "Going deeper in facial expression recognition using deep neural networks," in *2016 IEEE Winter Conference on Applications of Computer Vision (WACV)*, 2016. 2
- [25] E. Barsoum, C. Zhang, C. C. Ferrer, and Z. Zhang, "Training deep networks for facial expression recognition with crowdsourced label distribution," in *ACM International Conference on Multimodal Interaction*, 2016.
- [26] S. Li and W. Deng, "Reliable crowdsourcing and deep locality-preserving learning for expression recognition in the wild," in *IEEE Conference on Computer Vision and Pattern Recognition*, 2017. 2, 3
- [27] A. Dosovitskiy, L. Beyer, and A. Kolesnikov, "An image is worth 16x16 words: Transformers for image recognition at scale," in *International Conference on Learning Representations*, 2021. 2
- [28] Z. Zhao and Q. Liu, "Former-dfer: Dynamic facial expression recognition transformer," in *Proceedings of the 29th*

ACM International Conference on Multimedia, pp. 1553–1561, 2021.

- [29] F. Ma, B. Sun, and S. Li, “Logo-former: Local-global spatio-temporal transformer for dynamic facial expression recognition,” in *Proceedings of the IEEE International Conference on Acoustics, Speech and Signal Processing (ICASSP)*, pp. 1–5, IEEE, 2023. [2](#)
- [30] S. Hochreiter and J. Schmidhuber, “Long short-term memory,” *Neural Computation*, 1997. [2](#)
- [31] C. Lea, M. Flynn, and R. Vidal, “Temporal convolutional networks for action segmentation,” in *IEEE Conference on Computer Vision and Pattern Recognition*, 2017.
- [32] A. Vaswani, N. Shazeer, and N. Parmar, “Attention is all you need,” in *Advances in Neural Information Processing Systems*, 2017.
- [33] S. Poria, E. Cambria, R. Bajpai, and A. Hussain, “A review of affective computing: From unimodal analysis to multimodal fusion,” *Information Fusion*, vol. 37, pp. 98–125, 2017.
- [34] Y.-H. H. Tsai, S. Bai, P. P. Liang, J. Z. Kolter, L.-P. Morency, and R. Salakhutdinov, “Multimodal transformer for unaligned multimodal language sequences,” in *Proceedings of the 57th Annual Meeting of the Association for Computational Linguistics*, pp. 6558–6569, 2019.
- [35] J.-H. Kim, N. Kim, M. Hong, and C. S. Won, “Advanced facial analysis in multi-modal data with cascaded cross-attention based transformer,” in *Proceedings of the IEEE/CVF Conference on Computer Vision and Pattern Recognition (CVPR) Workshops*, pp. 7870–7877, 2024. [2](#), [3](#)
- [36] J. Yu, Z. Wei, Z. Cai, G. Zhao, Z. Zhang, Y. Wang, G. Xie, J. Zhu, W. Zhu, Q. Liu, and J. Liang, “Exploring facial expression recognition through semi-supervised pre-training and temporal modeling,” in *Proceedings of the IEEE/CVF Conference on Computer Vision and Pattern Recognition (CVPR) Workshops*, pp. 4880–4887, 2024. [2](#), [3](#)
- [37] J. A. Russell, “A circumplex model of affect,” *Journal of Personality and Social Psychology*, vol. 39, no. 6, pp. 1161–1178, 1980. [3](#)
- [38] D. Kollias, P. Tzirakis, A. Cowen, S. Zafeiriou, I. Kotsia, E. Granger, M. Pedersoli, S. Bacon, A. Baird, C. Gagne, C. Shao, G. Hu, S. Belharbi, and M. H. Aslam, “Advancements in affective and behavior analysis: The 8th abaw workshop and competition,” in *Proceedings of the IEEE/CVF Conference on Computer Vision and Pattern Recognition (CVPR) Workshops*, pp. 5611–5622, June 2025. [6](#)